ORIGINAL ARTICLE

Conservative analysis of *Synaptopodin-2* intron sense-overlapping lncRNA reveals its novel function in promoting muscle atrophy

Jianjun Jin[1,2,3], Mengmeng Du[1,2], Jian Wang[1,2], Yubo Guo[1,2], Jiali Zhang[1,2], Hao Zuo[1,2], Yunqing Hou[1,2], Shanshan Wang[1,2], Wei Lv[1,2], Wei Bai[1,2], Jin Wang[1,2], Xizhen Zhan[1,2], Yaxin Peng[1,2], Qian Tong[1,2], Jin Chai[1,2], Zaiyan Xu[1,4]* & Bo Zuo[1,2,5,6,7,8]* (iD)

[1]*Key Laboratory of Swine Genetics and Breeding of the Ministry of Agriculture and Rural Affairs, Huazhong Agricultural University, Wuhan, China;* [2]*Key Laboratory of Agriculture Animal Genetics, Breeding and Reproduction of the Ministry of Education, Huazhong Agricultural University, Wuhan, China;* [3]*Key Laboratory of Animal Genetics, Breeding and Reproduction of Shaanxi Province, Laboratory of Animal Fat Deposition and Muscle Development, College of Animal Science and Technology, Northwest A&F University, Yangling, China;* [4]*Department of Basic Veterinary Medicine, College of Veterinary Medicine, Huazhong Agricultural University, Wuhan, China;* [5]*Hubei Hongshan Laboratory, Wuhan, China;* [6]*The Cooperative Innovation Center for Sustainable Pig Production, Wuhan, China;* [7]*Shenzhen Institute of Nutrition and Health, Huazhong Agricultural University, Wuhan, China;* [8]*Shenzhen Branch, Guangdong Laboratory for Lingnan Modern Agriculture, Genome Analysis Laboratory of the Ministry of Agriculture, Agricultural Genomics Institute at Shenzhen, Chinese Academy of Agricultural Sciences, Shenzhen, China*

Abstract

Background   Dissection of the regulatory pathways that control skeletal muscle development and atrophy is important for the treatment of muscle wasting. Long noncoding RNA (lncRNA) play important roles in various stages of muscle development. We previously reported that *Synaptopodin-2* (*SYNPO2*) intron sense-overlapping lncRNA (*SYISL*) regulates myogenesis through an interaction with enhancer of zeste homologue 2 (EZH2). However, it remains unclear whether *SYISL* homologues exist in humans and pigs, and whether the functions and mechanisms of these homologues are conserved among species.

Methods   Bioinformatics, cell fractionation, and quantitative real-time polymerase chain reaction (qRT-PCR) analyses were used for the identification and molecular characterization of *SYISL* homologues in humans and pigs. Effects on myogenesis and muscle atrophy were determined via loss-of-function or gain-of-function experiments using C2C12 myoblasts, myogenic progenitor cells, dexamethasone (DEX), and aging-induced muscle atrophy models. RNA pulldown, RNA immunoprecipitation, dual luciferase reporting, and co-transfection experiments were used to explore the mechanisms of *SYISL* interactions with proteins and miRNAs.

Results   We identified *SYISL* homologues in humans (designated *hSYISL*) and pigs (designated *pSYISL*). Functional experiments demonstrated that *hSYISL* and *pSYISL* regulate myogenesis through interactions with EZH2. Interestingly, we showed that *SYISL* functions to regulate muscle atrophy and sarcopenia through comparative analysis. *SYISL* is significantly up-regulated after muscle atrophy ($P < 0.01$); it significantly promotes muscle atrophy in DEX-induced muscle atrophy models ($P < 0.01$). *SYISL* knockdown or knockout alleviates muscle atrophy and sarcopenia in DEX-induced and aged mice. The tibialis anterior (TA) muscle weight of 3-month-old wild-type (WT) mice decreased by 33.24% after DEX treatment ($P < 0.001$), while the muscle weight loss of 3-month-old *SYISL* knockout mice was only 18.20% after DEX treatment ($P < 0.001$). *SYISL* knockout in 18-month-old WT mice significantly increased the weights of quadriceps (Qu), gastrocnemius (Gas), and TA muscles by 10.45% ($P < 0.05$), 13.95% ($P < 0.01$), and 24.82% ($P < 0.05$), respectively. Mechanistically, *SYISL* increases the expression levels of the muscle atrophy genes *forkhead box protein O3a* (*FoxO3a*), *muscle ring finger 1* (*MuRF1*), and *muscle atrophy-related F-box* (*Atrogin-1*) via sponging of *miR-23a-3p/miR-103-3p/miR-205-5p* and thus promotes muscle atrophy. Additionally, we verified that human *SYISL* overexpression in muscles of 18-month-old WT mice significantly decreased the weights of Gas, Qu, and TA muscles by 7.76% ($P < 0.01$), 12.26% ($P < 0.05$), and 13.44% ($P < 0.01$), respectively, and accelerates muscle atrophy through conserved mechanisms.

Conclusions   Our results identify *SYISL* as a conserved lncRNA that modulates myogenesis in mice, pigs, and humans. We also demonstrated its previously unknown ability to promote muscle atrophy.

Keywords   *SYISL*; Myogenesis; Muscle atrophy; miRNA sponging

*Correspondence to: Bo Zuo, College of Animal Science and Technology, Huazhong Agricultural University, Wuhan, China. Email: zuobo@mail.hzau.edu.cn; Zaiyan Xu, Department of Basic Veterinary Medicine, College of Veterinary Medicine, Huazhong Agricultural University, Wuhan, China. Email: xuzaiyan@mail.hzau.edu.cn
Jianjun Jin and Mengmeng Du contributed equally to the manuscript.

Introduction

Normal muscle development is controlled by multiple strict regulatory networks and disordered regulation of gene expression leads to various muscle diseases.[1,2] Muscle atrophy or sarcopenia occurs in specific muscles under conditions of inactivity, denervation, aging, and diseases,[3,4] and it is characterized by progressive and extensive loss of skeletal muscle mass and strength, as well as a decrease in protein synthesis.[5] Muscle atrophy leads to protein degradation through activation of two proteolytic systems: the ubiquitin-proteasome system (UPS) and the autophagy-lysosome system.[2,6] Most muscle proteins are degraded by ubiquitin ligases in the UPS system, such as *MuRF1* and *Atrogin-1*, which are the core components of the UPS[7]; these proteins are excellent markers of muscle atrophy.[5,8] Autophagy is another proteolysis system with a crucial role in the turnover of specific cell organelles (e.g. mitochondria) and abnormal proteins.[6,9,10] Activation of the UPS and autophagy during muscle atrophy is regulated by multiple genes and signalling pathways, including the insulin-like growth factor-1 (IGF-1)-phosphatidylinositol3-kinase (PI3K)-protein kinase B (PKB; also called Akt)-forkhead box protein O (FoxO), nuclear factor κB (NF-κB) signalling pathways, and so on.[5,11] Recent studies have revealed that FoxOs promote the expression of atrophy-related and autophagy-related genes, which then activate the UPS and autophagy, leading to muscle atrophy.[12,13] Most eukaryotic genome contents comprise non-coding RNA; only a few regions represent protein-coding genes. Long noncoding RNAs (LncRNAs) have emerged as crucial regulators of numerous biological processes.[14,15] Although lncRNAs have low conservation among species, particularly in terms of nucleotide sequences, many lncRNAs (e.g. *Neat1*,[16] *Linc-YY1*,[17] *H19*,[18] and *lncMGPF*[19]) exhibit cross-species conservation of genomic positions, functions, and regulatory mechanisms. We previously showed that *Synaptopodin-2* (*SYNPO2*) intron sense-overlapping lncRNA (*SYISL*) promotes myoblast proliferation but inhibits myogenic differentiation. *SYISL* knockout (KO) in mice results in the increased muscle fibre density and muscle mass. Mechanistically, *SYISL* recruits polycomb repressive complex 2 (PRC2) to the promoters of the cell-cycle inhibitor gene *p21* and muscle-specific genes such as *myogenin* (*MyoG*), leading to H3K27 trimethylation and epigenetic silencing of target genes.[20] Bioinformatics analysis revealed that *AK021986* (renamed *hSYISL*) and *AK238214* (renamed *pSYISL*) are transcribed from the intron of the *SYNPO2* gene in humans and pigs, respectively. However, it is not clear whether the homologous transcripts of *SYISL* are functionally and mechanistically conserved in humans and pigs. In this study, we investigated the roles of human and pig *SYISL* homologue transcripts in muscle development and atrophy. Our results revealed that the functions of *SYISL* in myogenesis regulation are conserved among mice, pigs, and humans. Interestingly, comparative analysis of *SYISL* among mice, pigs, and humans revealed a novel function in promoting muscle atrophy. *SYISL* increases the expression levels of muscle atrophy genes (*FoxO3a*, *MuRF1*, and *Atrogin-1*) via sponging of *miR-23a-3p*/*miR-103-3p*/*miR-205-5p*, activates the UPS and autophagy-lysosome system, and thus aggravates muscle atrophy. Our findings highlight the conservation of *SYISL* among different species and its potential as a therapeutic target for sarcopenia.

Materials and methods

An extended materials and methods section can be found online in the Supporting Information.

Animals

All C57BL/6J wild-type (WT) mice and *SYISL* KO mice used for the study were from the Experimental Animal Center of Huazhong Agricultural University. *SYISL* KO mice were originally generated by our lab.[20] All pigs were from the experimental pig farm of Huazhong Agricultural University.

Measurement of phenotypes

The whole leg, gastrocnemius (Gas), tibialis anterior (TA), and quadriceps (Qu) muscles of KO and WT mice were collected and weighed. Data were normalized to the body weight (mg/g). The strength test was performed using a grip strength metre (BIO-GS3; Bioseb, France).

Dual-luciferase reporter assay

The sequences of 3ꞌuntranslated regions (3ꞌUTRs) of *MuRF1*, *Atrogin-1*, and *FoxO3a* containing *miR-23a-3p*, *miR-103-3p*, and *miR-205-5p* binding sites, and *SYISL*, *hSYISL*, and *pSYISL* with unmutated or mutated binding sites were cloned into the pmirGLO Dual-Luciferase miRNA Target Expression Vectors (E1330; Promega, USA), respectively. Those reporter vectors were transfected or co-transfected into C2C12 or HeLa cells using Lipofectamine 2000 and then tested according to a previously published method.[21]

Muscle atrophy models

For dexamethasone (DEX)-induced muscle atrophy model, 3-month-old WT and *SYISL* KO mice were intraperitoneally injected with DEX (HY-14648; 25 μg/g weight, MedChemExpress, China) once a day for 10 days. For the starvation-induced muscular atrophy model, 3-month-old WT mice were fasted for 5 days but given free water. For the sarcopenia model, WT mice with the same birth date and conditions grew up to 18 months old.

Cell immunofluorescence staining

Cell immunofluorescence staining was performed according to the previous literature.[20] Antibodies included a primary antibody MyHC (sc-376157; 1:200; Santa Cruz Biotechnology, USA) and a secondary antibody (A0521; goat anti-mouse CY3; Beyotime Biotechnology, China). The images were visualized with a fluorescence microscope (IX51-A21PH; Olympus, Japan).

Statistical analysis

Statistical analyses among different groups were performed using unpaired or paired Student's *t*-test. For all analyses, $^*P < 0.05$ and $^{**}P < 0.01$ were considered to be statistically significant. All data were presented as mean ± standard deviation (SD).

Results

SYNPO2 intron sense-overlapping lncRNA exhibits conserved genomic position and expression pattern among mice, pigs, and humans

Mouse *SYISL* is transcribed from the fourth intron of the *SYNPO2* gene and negatively regulates muscle growth.[20] To explore whether *SYISL* homologues occur in pigs and humans, we searched for lncRNAs transcribed from the intron of *SYNPO2* in human and pig genomes using the University of California Santa Cruz database (UCSC database). We identified transcript *AK238214* (i.e. *pSYISL*) in pigs; it is transcribed from the first intron of the pig *SYNPO2* gene. We also identified transcript *AK021986* (i.e. *hSYISL*) in humans; it is transcribed from the fourth intron of the human *SYNPO2* gene (*Figure* S1A). Bioinformatics analysis showed that they have low coding potential (*Figure* S1B), short conserved sequences with *SYISL* (*Figure* S1C), and conserved loop structures that may bind to proteins (*Figure* S1D). In our previous study, we showed that *SYISL* could interact with enhancer of zeste homologue 2 (EZH2) to form a larger structure. Therefore, we predicted the capacities of *pSYISL* and *hSYISL* to bind EZH2 by using the machine learning classifier RNA-protein interaction prediction (RPISeq). Notably, EZH2 had high affinity for *SYISL*, *pSYISL*, and *hSYISL* (*Figure* S1E). Moreover, RegRNA2 prediction of miRNA binding sites showed that mouse, pig, and human *SYISL* contain 49, 108, and 68 potential miRNA-binding sites, respectively, among which binding sites for five miRNAs (*miR-103-3p*, *miR-23a-3p*, *miR-24a-3p*, *miR-27a-3p*, and *miR-205-5p*) were common (*Figure* 1A). Binding interactions with EZH2 and *SYISL*-specific miRNAs were confirmed via subsequent analysis.

Next, we examined the subcellular distribution and expression profiles of *hSYISL* and *pSYISL*. Cell fractionation assays demonstrated that *pSYISL* is mainly localized to the nuclei, while *hSYISL* is localized to both nuclei and cytoplasm in proliferating myoblasts (D0), myotubes differentiated for 6 days (D6), and D6 atrophy myotubes after DEX treatment (D6 + DEX) (*Figure* 1B,C); the subcellular localizations of *hSYISL* and *pSYISL* were confirmed by RNA FISH (*Figure* S1F, G). Our previous lncRNA database results showed that *hSYISL* is highly expressed in human muscles.[20] Further analysis of the enrichment pathways of genes co-expressed with *hSYISL* in the AnnoLnc2 database indicated that *hSYISL* may be involved in pathways related to muscle development and muscle contraction (*Figure* S1H). Similar to mouse and human *SYISL*, *pSYISL* was highly expressed in skeletal muscles (*Figure* 1D), and the expression levels of *hSYISL* and *pSYISL* increased with the differentiation of human skeletal muscle myoblasts and pig primary myoblasts, respectively (*Figure* 1E). Moreover, the expression of *pSYISL* increased during skeletal muscle growth after birth (*Figure* 1F; *Figure* S1I). Prediction of the binding sites of transcription factors showed that the *pSYISL* promoter region contains multiple potential binding sites of transcription factors such as *MyoD*, *MyoG*, *Myf5*, *MEF2C*, and *FoxO3*, which are involved in embryonic and postnatal muscle development, as well as muscle atrophy (*Figure* S1J). Therefore, we speculated that the increased expression levels of *pSYISL* after birth and during myogenic differentiation may be induced by these transcription factors. These hypotheses need further validation in future.
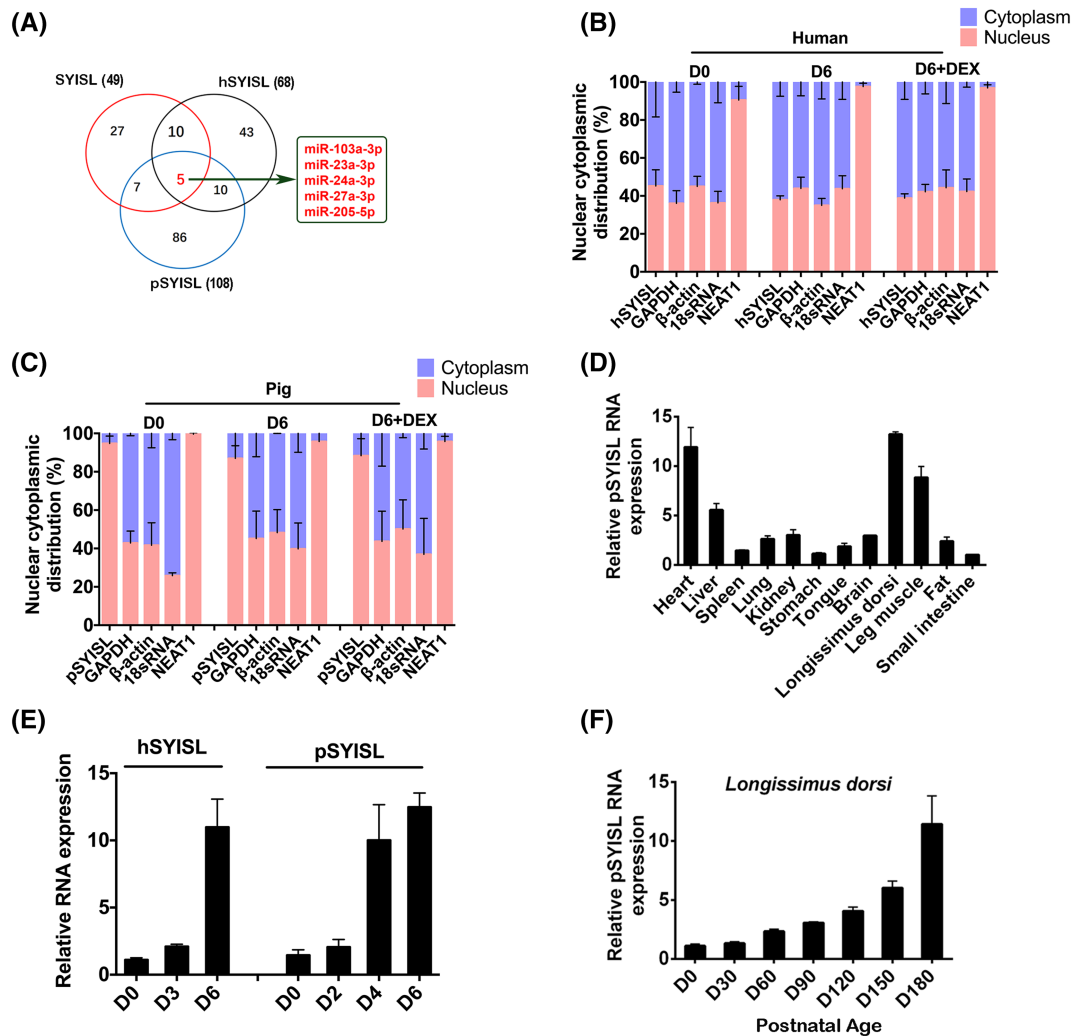
Figure 1 *SYNPO2* intron sense-overlapping lncRNA exhibits conserved genomic position, subcellular distribution, and expression pattern among mice, pigs, and humans. *(A)* Venn diagram shows potential miRNAs that can binding to *SYISL*, *hSYISL*, and *pSYISL*. The overlapping results show that *miR-103-3p*, *miR-23a-3p*, *miR-24a-3p*, *miR-27a-3p*, and *miR-205-5p* are the predicted common miRNAs. *(B,C)* qRT-PCR results showing the distribution of *pSYISL* and *hSYISL* in the cytoplasm and nucleus of proliferating myoblasts (D0), myotubes differentiated for 6 days (D6), and D6 atrophy myotubes after dexamethasone (DEX) treatment (D6 + DEX). *(D)* qRT-PCR results show that *pSYISL* is highly expressed in muscle tissues including the longissimus dorsi, leg muscle, and heart. *(E)* qRT-PCR results show that the expression levels of *hSYISL* and *pSYISL* gradually increase during myoblast differentiation in human skeletal muscle myoblasts and pig primary myoblasts, respectively. *(F)* qRT-PCR results show that *pSYISL* expression level gradually increases during postnatal longissimus dorsi muscle development. The relative RNA levels are normalized to GAPDH. The data are presented as mean ± SD.

In summary, we concluded that *SYISL* exhibits conservation of its genomic position and expression pattern among mice, pigs, and humans.

Regulation of myogenesis by SYNPO2 intron sense-overlapping lncRNA is conserved in pigs and humans

To explore whether the *SYISL* myogenesis function is conserved in pigs and humans, we used loss-of-function and gain-of-function experiments to study the functions of *hSYISL* and *pSYISL*. Compared with the control, overexpression of

hSYISL and *pSYISL* promoted the proliferation capacities of human skeletal muscle myoblasts (*Figure* 2A; *Figure* S2A, C), and pig primary myoblasts (*Figure* 2B; *Figure* S2B,D), respectively, while *hSYISL* and *pSYISL* knockdown inhibited myoblast proliferation (*Figure* S2E–I). Furthermore, we investigated the influences of *hSYISL* and *pSYISL* on myoblast differentiation in human skeletal muscle myoblasts and pig primary myoblasts, respectively. The results showed that overexpression of *hSYISL* and *pSYISL* inhibited myoblast differentiation (*Figure* 2C,D; *Figure* S2J–M), while knockdown of *hSYISL* and *pSYISL* promoted myoblast differentiation (*Figure* S2N–Q). These results were consistent with our previous findings in mice.[20] To investigate whether *pSYISL* and
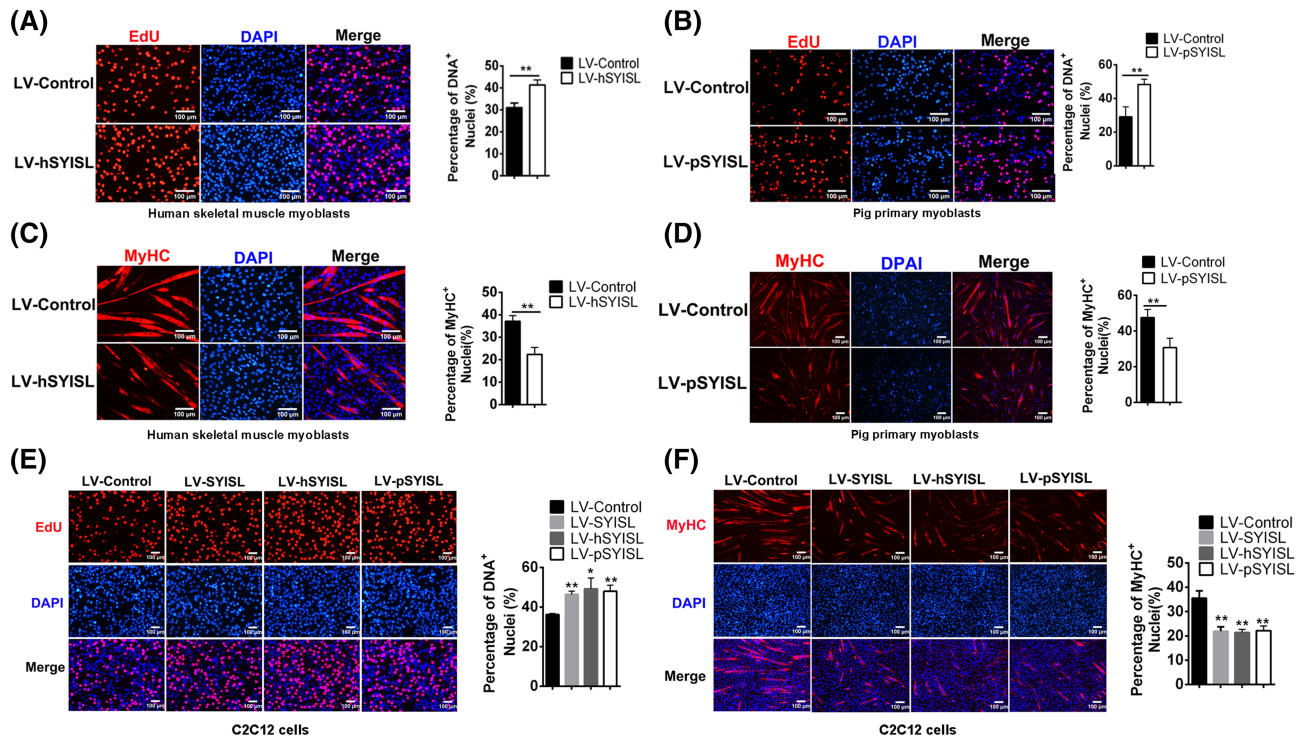
Figure 2 Regulation of myogenesis by *SYNPO2* intron sense-overlapping lncRNA is conserved in pigs and humans. *(A,B)* Representative photographs of EdU staining in human skeletal muscle myoblasts and pig primary myoblasts and quantification show that overexpression of *hSYISL* in human skeletal muscle myoblasts *(A)* and *pSYISL* in pig primary myoblasts *(B)* can significantly increase myoblast proliferation. Nuclei are stained with DAPI, scale bars, 100 μm. *(C,D)* Representative photographs of MyHC immunofluorescence staining and quantification show that *hSYISL* and *pSYISL* overexpression inhibits myoblasts differentiation in human skeletal muscle myoblasts *(C)* and pig primary myoblasts *(D)*, respectively. Positively stained cells are quantified; nuclei are stained with DAPI. Scale bars, 100 μm. *(E)* Representative photographs of EdU staining and quantification show that *hSYISL*, *SYISL*, and *pSYISL* overexpression in C2C12 cells significantly increases EdU incorporation and cell proliferation. Nuclei are stained with DAPI. Scale bars, 100 μm. *(F)* Representative photographs of immunofluorescence staining for MyHC and quantification show that overexpression of *hSYISL*, *SYISL*, and *pSYISL* in C2C12 cells significantly inhibits myoblast differentiation. Nuclei are stained with DAPI. Scale bars, 100 μm. The data of three independent experiments are presented as mean ± SD; *$P < 0.05$, **$P < 0.01$. N.S. indicates statistical non-significance.

hSYISL exhibit cross-species functional conservation, we expressed *pSYISL* and *hSYISL* in C2C12 cells. The results showed that overexpression of *hSYISL* and *pSYISL* significantly promoted cell proliferation (*Figure* 2E; *Figure* S3A–C) and inhibited C2C12 cell differentiation (*Figure* 2F; *Figure* S3D–F), which was consistent with the effects of *SYISL* overexpression. We further examined the expression of *SYNPO2* and no significant change was found after overexpression of *hSYISL* and *pSYISL* (*Figure* S3G–J). Taken together, these results demonstrated that *SYISL* functions to regulate myogenesis in mice, pigs, and humans.

Next, we further verified the conservative functional of *hSYISL* and *pSYISL* on muscle growth and development in 1-month-old WT mice. Compared with control group, overexpression of *hSYISL* and *pSYISL* in mice muscles significantly reduced the muscle sizes and weights (*Figure* 3A,B; *Figure* S4A, B). EGFP immunofluorescence staining in TA muscles showed that the infection efficiency of lentivirus was 100% in both control and overexpression groups, excluding the effect of transfection efficiency on muscle growth (*Figure* S4C,D).

Moreover, haematoxylin and eosin (H&E) and Lamin immunofluorescence staining showed that *hSYISL* or *pSYISL* overexpression significantly reduced the cross-sectional areas of the Qu, Gas, and TA muscles (*Figure* 3C,D; *Figure* S4E,F). Quantification of the number of centrally localized nuclei after infection showed that there were no centrally localized nuclei after infection of lentivirus, indicating the reduction in muscle size is due to the reduced muscle growth, not to the myopathy. MyoD and MyoG immunofluorescence staining in muscles showed that overexpression of *hSYISL* significantly decreased the number of MyoG positive cells but did not significantly affect the number of MyoD positive cells in the interstitial cell matrix (*Figure* S4G,H); these results were also confirmed by Western blotting (*Figure* S4I,J). Then, we further verified the functional conservation of *pSYISL* during pig muscle development, the inhibiting effects of *pSYISL* on pig muscle growth, and myogenic differentiation were consistent with the results in mice (*Figure* 3E,F; *Figure* S4K,L). These results indicated that *hSYISL* and *pSYISL* inhibit muscle growth and development *in vivo*.
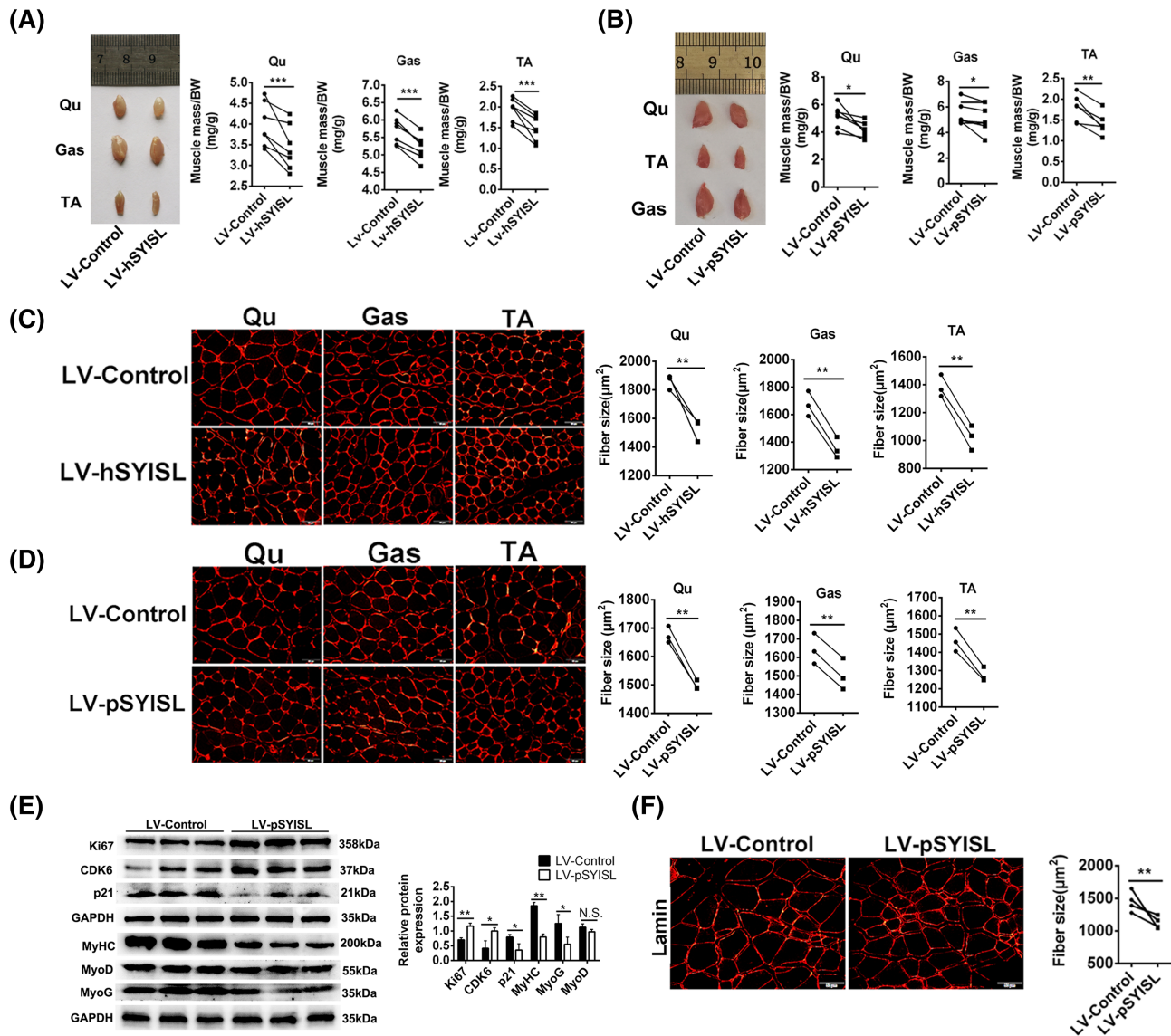
Figure 3 Human and pig *SYNPO2* intron sense-overlapping lncRNA inhibit the muscle growth and development *in vivo*. *(A,B)* Representative photographs of the muscle mass for quadriceps (Qu), gastrocnemius (Gas), and tibialis anterior (TA) of 1-month-old mice injected with lentivirus-mediated *hSYISL* overexpression (LV-*hSYISL*) vector *(A)* or *pSYISL* overexpression (LV-*pSYISL*) vector *(B)*. Quantification of six independent experiments shows that lentivirus-mediated *hSYISL (A)* or *pSYISL (B)* overexpression significantly decreases the weights of Gas, TA, and Qu muscles. *P* values are determined by paired *t*-test. Data are normalized to the body weight (BW) (mg/g). *(C,D)* Representative images of Lamin immunofluorescence staining for Qu, Gas, and TA muscles of mice. Quantification of three independent experiments indicates that lentivirus-mediated *hSYISL (C)* or *pSYISL (D)* overexpression in muscles of mice significantly decreases the average cross-sectional areas of individual myofibre. At least 150 myofibres are analysed in an independent experiment. Scale bar, 50 μm. *(E)* Western blotting results of pig biceps femoris muscles show that overexpression of *pSYISL* significantly increases the expression of Ki67 and CDK6 and decreases the protein expression levels of MyoG, MyHC, and p21 but does not affect MyoD expression. *(F)* Representative images of Lamin immunofluorescence staining for the left and right biceps femoris muscles of 1-month-old piglets injected with LV-*pSYISL* vector or LV-control vector. Quantification of four independent experiments shows that *pSYISL* overexpression decreases average cross-sectional areas of individual myofibre. At least 150 myofibres are analysed in an independent experiment. Scale bar, 50 μm. The relative protein levels are normalized to GAPDH. The data of three independent experiments are presented as mean ± SD; *$P < 0.05$, **$P < 0.01$. N.S. indicates statistical non-significance.

We previously verified that *SYISL* regulates myogenesis and inhibits the expression of target genes such as *p21*, *MyoG*, and *MyHC* by recruiting EZH2/H3K27me3 to its target gene promoters; it has been unclear whether this mechanism is conserved in other species. Therefore, we investigated the conservation of this mechanism in pig primary myoblasts. RNA pulldown and immunoprecipitation results confirmed the interaction between EZH2 and *pSYISL* (*Figure* S5A,B),

and *pSYISL* overexpression significantly increased the enrichment of H3K27me3 at the proliferation and differentiation stages (*Figure* S5C). Chromatin immunoprecipitation (ChIP)-quantitative real-time polymerase chain reaction (qRT-PCR) results showed that *pSYISL* overexpression could significantly increase the binding of EZH2 and H3K27me3 to the *p21*, *MyoG*, and *myosin heavy chain 4* (*MyH4*) gene promoters (*Figure* S5D,E); knockdown of *pSYISL* could significantly reduce these binding capacities (*Figure* S5F,G). These results suggested that the molecular mechanism whereby *SYISL* regulates myogenesis via EZH2/H3K27me3 is conserved.

Comparative analysis of SYNPO2 intron sense-overlapping lncRNA among mice, pigs, and humans reveals its novel function in promoting muscle atrophy

The bioinformatics analysis described above showed that the overlapping miRNAs among mice, pigs, and humans were *miR-103-3p*, *miR-23a-3p*, *miR-24a-3p*, *miR-27a-3p*, and *miR-*205-5p. Dual luciferase reporter experiments and qRT-PCR results showed that *miR-103-3p*, *miR-23a-3p*, and *miR-205-5p* could simultaneously bind to *SYISL*, *pSYISL*, and *hSYISL* and significantly decreased the expression level of *SYISL* (*Figure* 4A,B; *Figure* S6A,B). We verified the binding of *SYISL* to Ago2 via RNA immunoprecipitation (*Figure* S6C), suggesting that *SYISL* functions via miRNA targeting. To confirm that these three miRNAs could directly bind to *SYISL*, *pSYISL*, and *hSYISL*, we performed dual luciferase reporter analysis of *SYISL* sequences containing the *miR-23a-3p*, *miR-103-3p*, and *miR-205-5p* binding sites, as well as their mutated binding sites. The results showed that overexpression of *miR-23a-3p*, *miR-103-3p*, and *miR-205-5p* significantly reduced the relative luciferase activities of *SYISL*, *pSYISL*, and *hSYISL*, respectively; no significant effects were observed upon mutation of these binding sites (*Figure* S6D–L). Among these three miRNAs, *miR-23a-3p* is known to regulate muscle atrophy.[22] Additionally, we performed pathway analysis of *SYISL* target genes using our reported gene chip results (GSE102087). The differentially expressed genes mainly participated in signalling pathways related to muscle atrophy, such as PI3K-Akt,
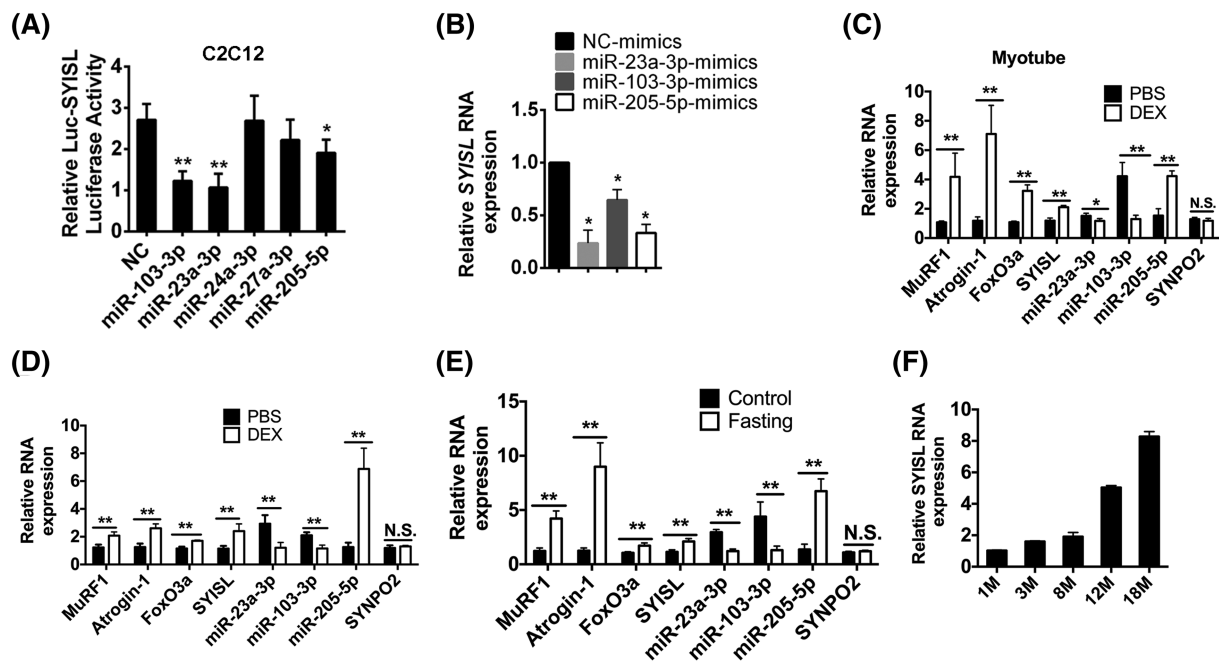
Figure 4 Comparative analysis of *SYNPO2* intron sense-overlapping lncRNA among mice, pigs, and humans reveals its potential function in promoting muscle atrophy. *(A)* Dual luciferase reporter assays show that overexpression of *miR-23a-3p*, *miR-103-3p*, and *miR-205-5p* can respectively reduce the dual luciferase activities of *SYISL*. *(B)* qRT-PCR results show that overexpression of *miR-23a-3p*, *miR-103-3p*, and *miR-205-5p* can reduce the expression level of *SYISL*, respectively. *(C)* qRT-PCR results show that DEX-induced myotube atrophy can increase the expression levels of *MuRF1*, *Atrogin-1*, *FoxO3a*, *SYISL*, and *miR-205-5p*, decrease the expression levels of *miR-23a-3p* and *miR-103-3p*, but does not affect the expression level of *SYNPO2*. *(D,E)* qRT-PCR results show that the expression levels of *MuRF1*, *Atrogin-1*, *FoxO3a*, *SYISL*, and *miR-205-5p* are up-regulated while *miR-23a-3p* and *miR-103-3p* are down-regulated in DEX-induced muscle atrophy *(D)* and starvation-induced muscle atrophy models *(E)*, while there is no significant change for the expression level of *SYNPO2*. Muscle atrophy and starvation-induced muscle atrophy are induced in 3-month-old wild-type mice by intraperitoneal injection of DEX for 10 days and fasted for 5 days, respectively. *(F)* qRT-PCR results show that the expression level of *SYISL* is up-regulated with aging. The relative miRNA levels are normalized to U6. The relative lncRNA and mRNA levels are normalized to GAPDH. The data of three independent experiments are presented as mean ± SD; *$P < 0.05$, **$P < 0.01$. N.S. indicates statistical non-significance.

FoxO, transforming growth factor-β (TGF-β), and ubiquitin-mediated proteolysis (*Figure* S6M,N). Therefore, we hypothesized that *SYISL* may be involved in muscle atrophy. To investigate this hypothesis, we examined the expression patterns of *SYISL* and related miRNAs in muscle atrophy models induced by aging, DEX treatment, and fasting. Among these models, the expression levels of *MuRF1*, *SYISL*, *miR-205-5p*, and other muscle atrophy-associated E3 ubiquitin ligases sig-

nificantly increased, while the expression levels of *miR-23a-3p* and *miR-103-3p* significantly decreased; no significant change for the expression of *SYNPO2* was observed in different muscle atrophy models (*Figure* 4C–E). Next, we examined the expression changes of these three miRNAs and *SYISL* at various stages of muscle growth. The expression levels of *SYISL* increased with age (*Figure* 4F), consistent with the pattern of *MuRF1* expression (*Figure* S6O). In addition, the expression
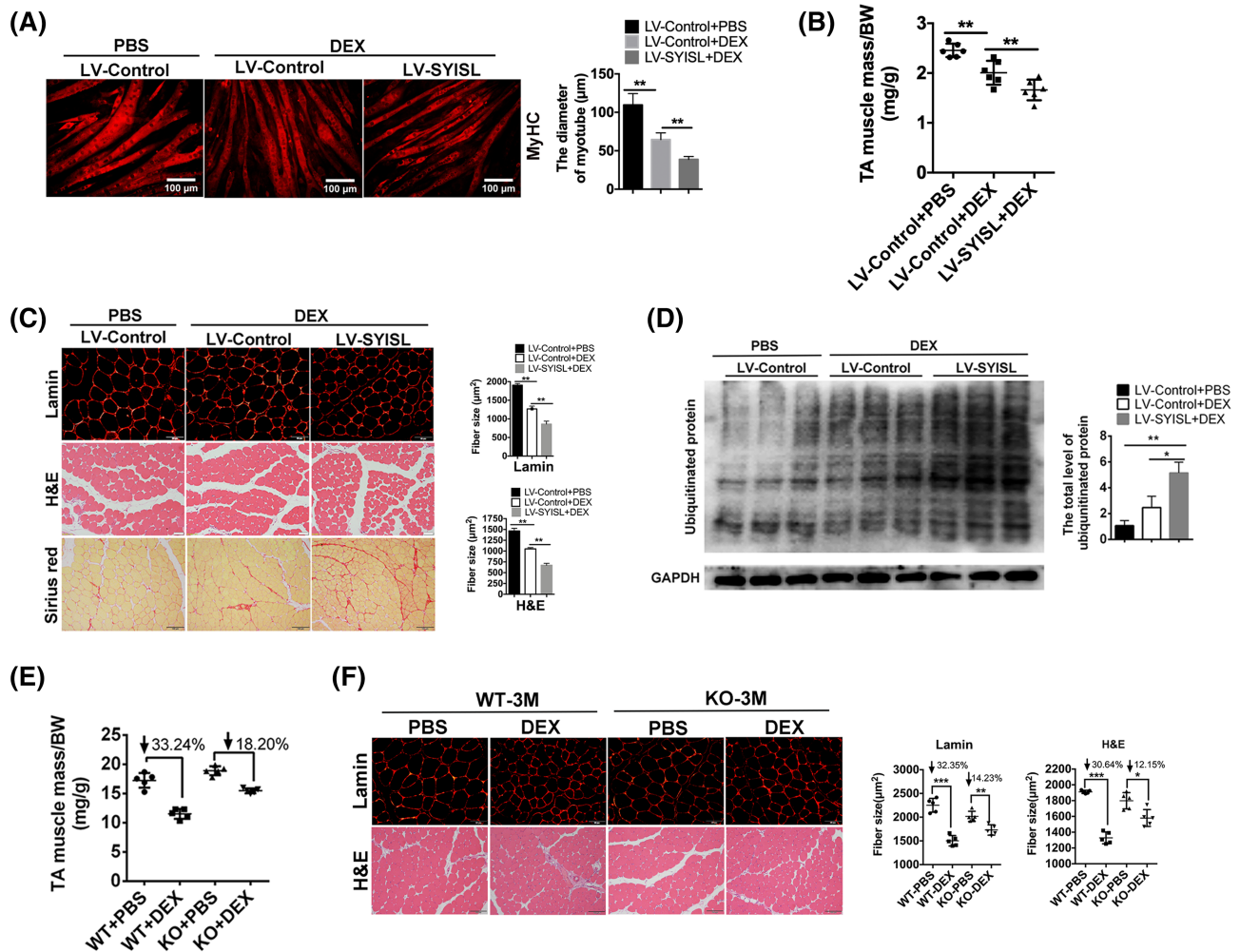
Figure 5 *SYNPO2* intron sense-overlapping lncRNA promotes myotube atrophy *in vitro* and aggravates DEX-induced muscle atrophy in mice. *(A)* Representative photographs of MyHC immunofluorescence for overexpression and knockdown *SYISL* in DEX-treated myotubes. Quantification of three independent experiments indicates that *SYISL* overexpression can further reduce the diameter of myotubes. Scale bar, 100 μm. *(B)* Quantification of six independent experiments shows that lentivirus-mediated *SYISL* overexpression can aggravate muscle weight loss caused by DEX-induced muscle atrophy. *(C)* Representative photographs of H&E, Lamin immunofluorescence, and Sirius red staining for TA muscles. Quantification of the three independent experiments shows that overexpression of *SYISL* further reduces the cross-sectional areas of TA muscles in DEX-induced muscle atrophy and increases the muscle fibrosis. At least 150 myofibres are analysed in an independent experiment. Scale bar, 50 μm (Lamin), 100 μm (H&E). *(D)* Western blotting results show that *SYISL* overexpression can further promote protein ubiquitination levels in DEX-induced muscular atrophy. Muscle atrophy is induced by intraperitoneal injection of DEX for 10 days in 3-month-old wild-type and KO mice, respectively. Intraperitoneal injection of PBS is used as control. *(E)* Quantification of five independent experiments shows that *SYISL* knockout counteracts the muscle weight loss caused by DEX-induced muscle atrophy. *(F)* Representative photographs of H&E and Lamin immunofluorescence staining for WT and KO TA muscles. Quantification of five independent experiments shows that knockout of *SYISL* alleviates muscle weight loss caused by DEX-induced muscle atrophy. At least 150 myofibres are analysed in an independent experiment. Scale bar, 50 μm (Lamin), 100 μm (H&E). The relative protein levels are normalized to GAPDH. The data of at least three independent experiments are presented as means ± SD. *$P < 0.05$, **$P < 0.01$. N.S. indicates statistical non-significance.

level of *miR-23a-3p* gradually decreased with age, and the expression of *miR-103-3p* remained stable during postnatal muscle development, while the expression level of *miR-205-5p* peaked at the age of 12 months (*Figure* S6P–R). These results suggest that *SYISL* is involved in the process of muscle atrophy.

To explore the roles of *SYISL* in muscle atrophy *in vitro*, we overexpressed and knocked down *SYISL* in C2C12 myotubes and myotubes after DEX treatment. The results showed that *SYISL* overexpression significantly increased the expression levels of *FoxO3a*, *Atrogin-1*, and *MuRF1* (*Figure* S7A,B); *SYISL* knockdown inhibited the expression of these genes (*Figure* S7C,D). Meanwhile, *SYISL* overexpression further promoted the expression of DEX-induced muscle atrophy genes (*Figure* S7E) and reduced the diameter of myotubes (*Figure* 5A). In contrast, *SYISL* knockdown alleviated DEX-induced myotube atrophy (*Figure* S7F,G). To determine the roles of *SYISL* in muscle atrophy *in vivo*, we performed *SYISL* KO, lentivirus-mediated overexpression, or knockdown experiments in DEX-induced muscle atrophy animal models. We found no significant differences in the expression levels of *FoxO3a*, *Atrogin-1*, and *MuRF1* between 3-month-old WT and *SYISL* KO mice (*Figure* S7H), mainly because 3-month-old mice do not exhibit an atrophy phenotype. Therefore, we treated 3-month-old mice with DEX to induce muscle atrophy. *SYISL* overexpression aggravated the DEX-induced loss of TA weight (*Figure* 5B). H&E, Lamin immunofluorescence, and Sirius red staining showed *SYISL* overexpression further reduced the TA muscle cross-sectional area and aggravated DEX-induced muscle fibrosis (*Figure* 5C). Moreover, *SYISL* overexpression significantly increased the expression of ubiquitinated proteins (*Figure* 5D), as well as the expression levels of *MuRF1*, *Atrogin-1*, and *FoxO3a* (*Figure* S7I). In contrast, *SYISL* knockdown alleviated DEX-induced TA muscle weights loss and atrophy phenotype and reduced the expression levels of DEX-induced muscle atrophy genes (*Figure* S7J–L). Quantification of the number of centrally localized nuclei after infection showed that there was no significant difference between control and *SYISL* overexpression (*Figure* S7M), or knockdown groups (*Figure* S7N), indicating the muscle atrophy by *SYISL* is not caused by the myopathy. To further characterize the contribution of *SYISL* to the regulation of DEX-induced muscle atrophy, 3-month-old WT and *SYISL* KO mice were treated with DEX to induce muscle atrophy. The results showed that TA muscle weight of 3-month-old WT mice decreased by 33.24% after DEX treatment ($P < 0.001$), while the muscle weight loss of 3-month-old *SYISL* KO mice was only 18.20% after DEX treatment ($P < 0.001$) (*Figure* 5E). *SYISL* KO significantly alleviated the DEX-induced reduction in muscle fibre cross-sectional area (*Figure* 5F) and inhibited the expression of muscle atrophy genes (*Figure* S7O). Taken together, these results indicated that *SYISL* aggravates DEX-induced muscle atrophy *in vivo* and *in vitro*.

Based on the results presented above, we investigated the roles of *SYISL* in muscle atrophy of aged mice. Compared with WT mice, 18-month-old *SYISL* KO mice had significantly

greater grasping force (*Figure* S8A), and *SYISL* KO significantly increased the weights of Qu, Gas, and TA muscles by 10.45% ($P < 0.05$), 13.95% ($P < 0.01$), and 24.82% ($P < 0.05$), respectively (*Figure* 6A). Compared with 18-month-old WT mice, the expression levels of *MuRF1*, *FoxO3a*, and *Atrogin-1* in 18-month-old *SYISL* KO mice were significantly decreased (*Figure* S8B,C), while no significant difference for the expression of *SYNPO2* was found (*Figure* S8D,E). Lamin immunofluorescence and Sirius red staining results showed that the degree of muscle atrophy in *SYISL* KO mice was significantly reduced, compared with WT mice (*Figure* 6B; *Figure* S8F). The results of Lamin immunofluorescence staining showed that the cross-sectional areas of muscle fibres were significantly smaller in *SYISL* KO mice than in WT mice at 3 and 8 months; they were significantly larger at 18 months (*Figure* 6C). Notably, no significant differences in the expression of *MuRF1*, *FoxO3a*, or *Atrogin-1* were found between 3-month-old *SYISL* KO and WT mice; however, their expression levels were significantly lower in 18-month-old *SYISL* KO mice than WT mice (*Figure* S8G). Next, we performed lentivirus-mediated *SYISL* interference experiments to determine whether *SYISL* knockdown in 18-month-old WT mice had a similar effect. The results showed *SYISL* knockdown significantly increased muscle sizes (*Figure* S8H) and weights (*Figure* 6D) and alleviated the muscle atrophy phenotype (*Figure* 6E; *Figure* S8I); it significantly decreased the expression levels of *MuRF1*, *FoxO3a*, and *Atrogin-1* (*Figure* 6F; *Figure* S8J). In conclusion, *SYISL* promotes muscle atrophy in aged mice; knockdown or KO of *SYISL* alleviates sarcopenia.

miR-23a-3p/miR-205-5p/miR-103-3p are required for SYNPO2 intron sense-overlapping lncRNA to regulate muscle atrophy and sarcopenia

miR-23a-3p inhibits muscle atrophy by targeting *MuRF1* and *Atrogin-1*.[22] Because the binding of *SYISL* to *miR-23a-3p* was verified by the results described above, we tested whether *SYISL* promotes muscle atrophy via *miR-23a-3p*. We introduced the 3′UTRs of *MuRF1* and *Atrogin-1* into dual luciferase reporter vectors and then co-transfected them with *SYISL* in C2C12 and HeLa cells. The results showed that *miR-23a-3p* significantly reduced the luciferase activities of Luc-*MuRF1*-3′UTR and Luc-*Atrogin-1*-3′UTR, while *SYISL* competed with *MuRF1*-3′UTR and *Atrogin-1*-3′UTR to combine with *miR-23a-3p*. Mutation of the binding sites between *SYISL* (*SYISL*-Mut) and *miR-23a-3p* eliminated this competitive activity (*Figure* S9A–D). Next, we injected a lentivirus-mediated *SYISL* overexpression vector with mutated binding sites of *SYISL* and *miR-23a-3p* into the leg muscles of 3-month-old mice, which were then treated with DEX to induce muscle atrophy. qRT-PCR and Western blotting results showed that overexpression of *SYISL*-Mut had no effect on the expression of *Atrogin-1*, although it promoted the expression of *FoxO3a* and *MuRF1* (*Figure* S9E,F). These results
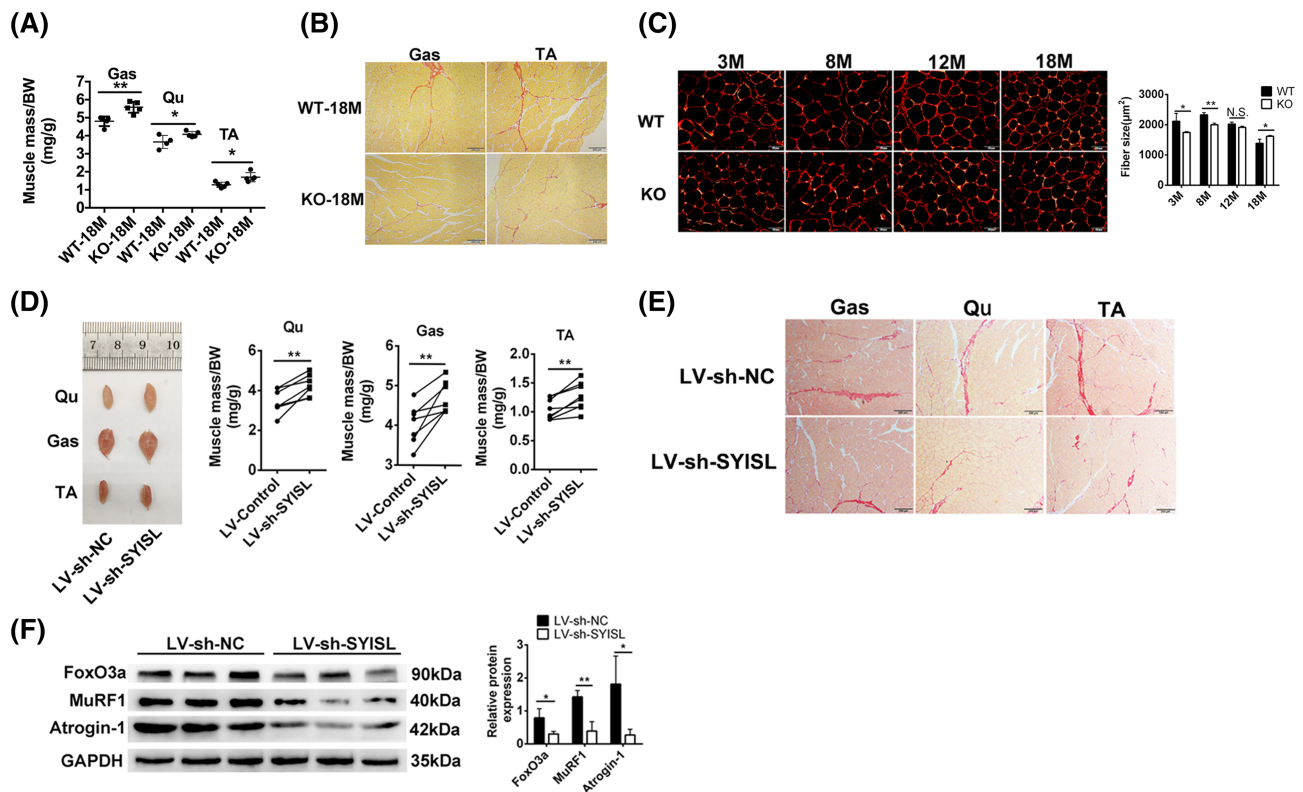
Figure 6 Knockdown or knockout of *SYNPO2* intron sense-overlapping lncRNA alleviates muscle atrophy in aged mice. *(A)* Quantification of five independent experiments for Qu, Gas, and TA muscles in 18-month-old KO and WT mice shows that compared with WT, knockout of *SYISL* can maintain muscle mass in aged mice. *(B)* Representative photographs of Sirius red staining for Gas and TA muscles show that *SYISL* knockout can significantly reduce muscle fibrosis in aged mice. *(C)* Representative photographs of Lamin immunofluorescence for TA muscles of 1-, 3-, 8-, 12-, and 18-month-old mice. Quantification of three independent experiments shows that *SYISL* knockout can maintain muscle fibre size during muscle atrophy. At least 150 myofibres are analysed in an independent experiment. Scale bars, 50 μm. *(D)* Representative photographs of Qu, Gas, and TA muscles of left and right legs of 18-month-old mice. Quantification of eight independent experiments shows that knockdown of *SYISL* increases muscle size and maintains muscle weight in aged mice. *(E)* Representative photographs of Sirius red staining show that *SYISL* knockdown reduces muscle fibrosis in aged mice. Scale bars, 200 μm. *(F)* Western blotting results show that knockdown of *SYISL* significantly decreases the expression levels of atrophy genes *FoxO3a*, *MuRF1*, and *Atrogin-1* in 18-month-old mice. The relative protein levels are normalized to GAPDH. The data of at least three independent experiments are presented as means ± SD. $*P < 0.05$, $**P < 0.01$. N.S. indicates statistical non-significance.

indicated that, in addition to the *miR-23a-3p*-mediated *Atrogin-1* and *MuRF1* pathway, *SYISL* promotes muscle atrophy through other pathways. As shown by the above experiments, *miR-103-3p* and *miR-205-5p* could directly bind to *SYISL*; the expression levels of *miR-103-3p* and *miR-205-5p* significantly varied after muscle atrophy. Moreover, RNAhybrid 2.12 prediction showed that *miR-103-3p* could bind to *MuRF1*, while *miR-205-5p* could bind to *MuRF1* and *FoxO3a* (*Figure* S9G). These results suggested that *miR-103-3p* and *miR-205-5p* may participate in *SYISL*-mediated regulation of muscle atrophy. Therefore, we selected *miR-103-3p* and *miR-205-5p* for further investigation. Firstly, we overexpressed these two miRNAs in C2C12 cells; the results showed that *miR-103-3p* significantly decreased the expression level of *MuRF1* (*Figure* 7A; *Figure* S9H), and *miR-205-5p* significantly reduced the expression levels of *MuRF1* and *FoxO3a* (*Figure* 7B; *Figure* S9I). Next, we introduced the 3′UTRs of *MuRF1* and *FoxO3a* into the dual lucif-

erase reporter vectors and then co-transfected them with *SYISL* or *SYISL*-Mut into C2C12 and HeLa cells. The results showed that *miR-103-3p* and *miR-205-5p* significantly reduced the luciferase activity of Luc-*MuRF1*-3′UTR; *SYISL* competed with *MuRF1*-3′UTR to combine with *miR-103-3p* and *miR-205-5p* (*Figure* 7C,D; *Figure* S9J,K,M,N,P,Q). In addition, *miR-205-5p* significantly reduced the luciferase activity of Luc-*FoxO3a*-3′UTR (*Figure* S9L,O); *SYISL* competed with *FoxO3a*-3′UTR to combine with *miR-205-5p* (*Figure* 7E; *Figure* S9R). Mutation of the binding sites between *SYISL* and *miR-103-3p* or *miR-205-5p* eliminated their competitive activities (*Figure* 7C–E; *Figure* S9J–R). These results suggested that *SYISL* functions as a sponge of *miR-103-3p* and *miR-205-5p* to promote the expression of *MuRF1* and *FoxO3a*, as well as muscle atrophy.

To determine whether *miR-23a-3p*, *miR-103-3p*, and *miR-205-5p* function cooperatively in *SYISL*-mediated regulation
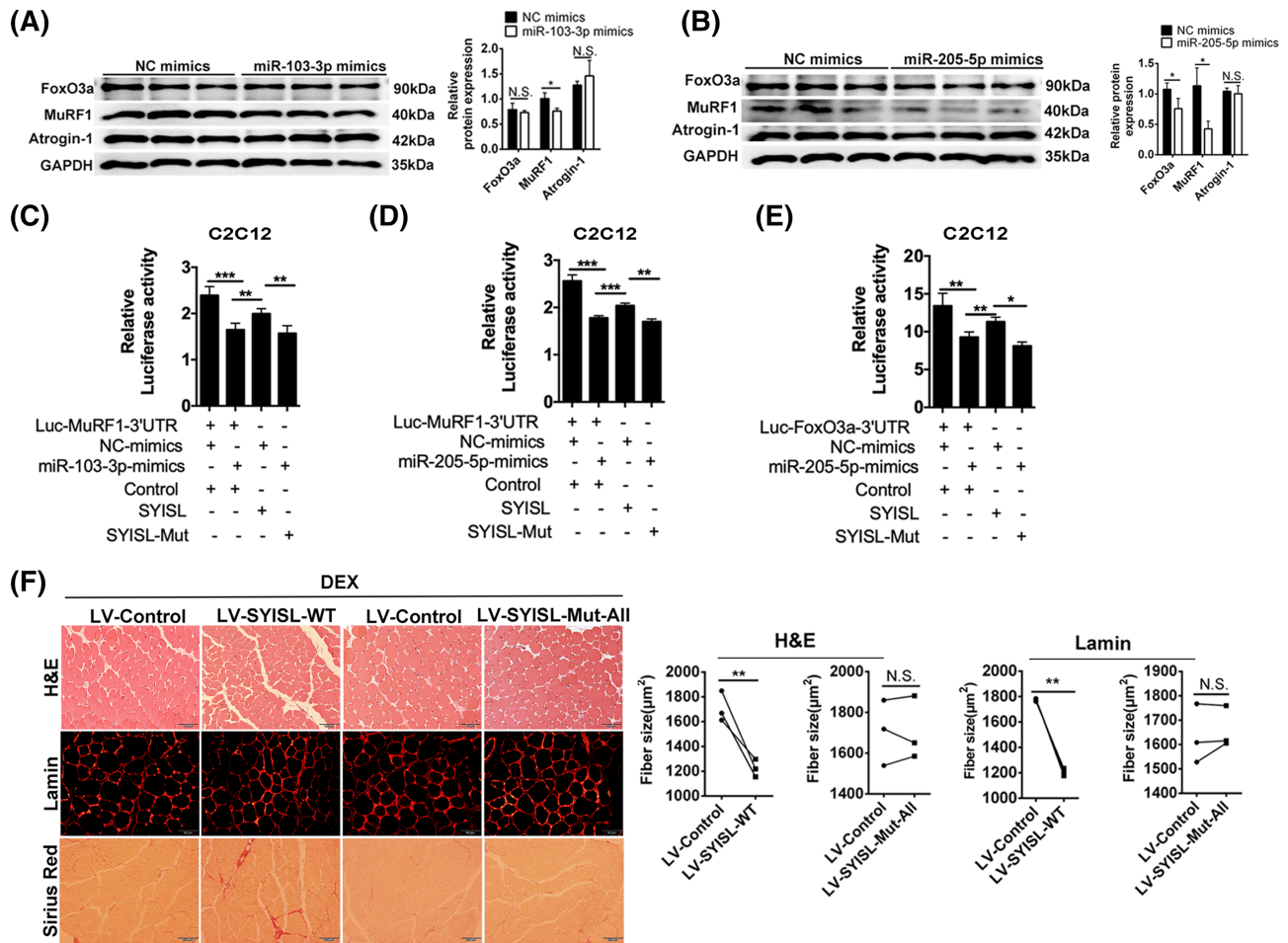
Figure 7 *miR-23a-3p/miR-205-5p/miR-103-3p* are required for *SYNPO2* intron sense-overlapping lncRNA to regulate muscle atrophy and sarcopenia. *(A)* Western blotting results show that overexpression of *miR-103-3p* inhibits the expression of *MuRF1* at protein levels in C2C12 myoblasts differentiated for 5 days. *(B)* Western blotting results show that in C2C12 myoblasts differentiated for 5 days, overexpression of *miR-205-5p* inhibits the expression of *MuRF1* and *FoxO3a* at protein levels. *(C,D)* Dual luciferase reporter assays of Luc-*MuRF1*-3ʹUTR in C2C12 myoblasts show that *SYISL* competes with *MuRF1*-3ʹUTR to combine with *miR-103-3p (C)* and *miR-205-5p (D)*. *(E)* Dual luciferase reporter assays of Luc-*FoxO3a*-3ʹUTR in C2C12 myoblasts show that *SYISL* competes with *FoxO3a*-3ʹUTR to combine with *miR-205-5p*. *(F)* Representative photographs of H&E staining and Lamin immunofluorescence staining for TA muscles. Quantification of three independent experiments shows that overexpression of *SYISL*-WT can further reduce muscle fibre cross-sectional areas and aggravate muscle fibrosis in DEX-induced muscle atrophy mice, while overexpression of *SYISL*-Mut-All has no significant effect on muscle fibre cross-sectional areas and muscle fibrosis. At least 150 myofibres are analysed in an independent experiment. Scale bar, 100 μm (H&E), 50 μm (Lamin). The relative protein levels are normalized to GAPDH. The data of at least three independent experiments are presented as means ± SD. *$P < 0.05$, **$P < 0.01$. N.S. indicates statistical non-significance.

of muscle atrophy, we mutated all binding sites of *SYISL* with *miR-23a-3p*, *miR-103-3p*, and *miR-205-5p* (*SYISL*-Mut-All) and then conducted lentivirus injection into the leg muscles of 3-month-old WT mice. The mice were intraperitoneally injected with DEX to induce muscle atrophy. The results showed that overexpression of *SYISL* significantly promoted the muscle atrophy, while overexpression of *SYISL*-Mut-All had no effect (*Figure* 7F; *Figure* S9S–X). Overall, these data indicated that *miR-23a-3p/miR-205-5p/miR-103-3p* are required for *SYISL*-mediated regulation of muscle atrophy.

Human SYNPO2 intron sense-overlapping lncRNA accelerates muscle atrophy via conserved mechanisms

To confirm that *hSYISL* has a conserved ability to promote muscle atrophy, we performed lentivirus-mediated *hSYISL* overexpression experiments in the muscles of 3-month-old DEX-induced mice and 18-month-old aged mice, respectively. There was no significant difference for the lentivirus infection efficiency between control and *hSYISL* overexpres-

sion groups (*Figure* S10A), which excluded the effect of transfection efficiency on muscle atrophy. As expected, overexpression of *hSYISL* aggravated the DEX-induced loss of TA weight (*Figure* S10B), further reduced the cross-sectional area of the TA muscles, and increased muscle fibrosis (*Figure* S10C). The expression levels of *MuRF1*, *Atrogin-1*, and *FoxO3a* were significantly increased after overexpression of *hSYISL* (*Figure* S10D). Quantification of the number of centrally localized nuclei after infection showed that there was no significant difference between control and *hSYISL* overexpression groups (*Figure* S10E), indicating the muscle atrophy by *hSYISL* overexpression is not caused by the myopathy. Similarly, *hSYISL* overexpression significantly decreased the weights of Gas, Qu, and TA muscles of 18-month-

old WT mice by 7.76% ($P < 0.01$), 12.26% ($P < 0.01$), and 13.44% ($P < 0.01$), respectively (*Figure* S10F). *hSYISL* overexpression also significantly decreased muscle fibre cross-sectional area and increased muscle fibrosis and expression levels of *MuRF1*, *Atrogin-1*, *FoxO3a*; no significant change for the expression level of *SYNPO2* was observed (*Figure* 8A; *Figure* S10G–I). To verify that *hSYISL* promotes muscle atrophy via sponging of *miR-23a-3p/miR-205-5p/miR-103-3p*, we performed dual luciferase reporter experiments and the results were consistent with the findings described above (*Figure* 8B–F; *Figure* S10J–L). Taken together, these results indicated that human *SYISL* has a conserved ability to promote muscle atrophy through interactions with *miR-23a-3p/miR-205-5p/miR-103-3p*.
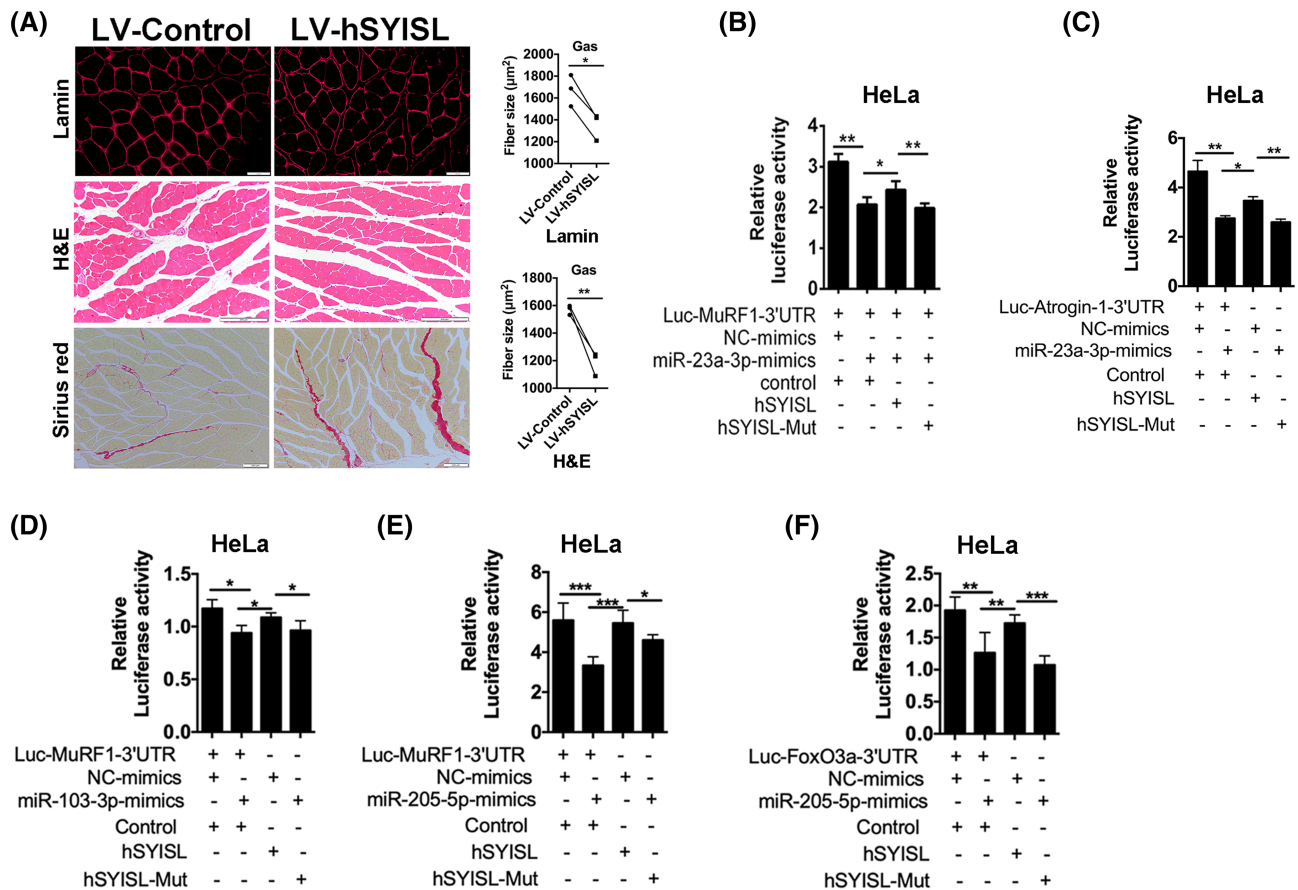
Figure 8 Human *SYNPO2* intron sense-overlapping lncRNA accelerates muscle atrophy via conserved mechanisms. *(A)* Representative photographs of H&E staining, Lamin immunofluorescence staining, and Sirius red staining for Gas muscles. Quantification of three independent experiments shows that overexpression of *hSYISL* reduces the muscle fibre cross-sectional area and increases the muscle fibrosis in 18-month-old WT mice. At least 150 myofibres are analysed in an independent experiment. Scale bar, 200 μm (H&E), 50 μm (Lamin), 200 μm (Sirius red). *(B,C)* Dual luciferase reporter assays results show that *hSYISL* can competitively bind to *miR-23a-3p* with *MuRF1 (B)* and *Atrogin-1 (C)* in HeLa cells. *(D,E)* Dual luciferase reporter assays of Luc-*MuRF1*-3ʹUTR in HeLa cells show that *hSYISL* competes with *MuRF1* to combine with *miR-103-3p (D)* and *miR-205-5p (E)*. *(F)* Dual luciferase reporter assays of Luc-*FoxO3a*-3ʹUTR in HeLa cells show that *hSYISL* competes with *FoxO3a* to combine with *miR-205-5p*. The data of at least three independent experiments are presented as means ± SD. *$P < 0.05$, **$P < 0.01$. N.S. indicates statistical non-significance.

Discussion

There is increasing evidence that lncRNAs are functionally conserved among species.[15,23,24] The functional conservation of lncRNAs among species can be explained as follows: lncRNAs have conserved binding domains and secondary or higher structures. For example, the 2D structure of the A region of *Xist* can recruit components of PRC2 that are needed for X-chromosome inactivation.[25] The 3D structure formed by the 98–153 nt sequence of the lncRNA *EDAL* is necessary for binding to EZH2 protein and subsequent *EDAL* function.[26] The binding sites of miRNAs require only 6–10 nt of base pairing, so most lncRNAs are highly conserved among species as molecular sponges of miRNAs. Our previous study showed that the binding sites of *miR-135-5p* on *lncMGPF* are highly conserved among humans, mice, and pigs.[19] Here, we identified conserved lncRNA transcripts of *SYISL* in humans and pigs. Sequence alignment revealed that their nucleotide sequences are dissimilar. However, bioinformatics analysis showed that *SYISL* can bind to EZH2 and has five common binding sites in mice, pigs, and humans. Further experiments verified that the regulation of myogenesis via *SYISL*–EZH2 interaction was conserved between pigs and humans. In addition, *miR-23a-3p/miR-205-5p/miR-103-3p* has vital roles in *SYISL*-mediated promotion of muscle atrophy among mice, humans, and pigs. These results indicate that *SYISL* is a conserved regulator of myogenesis and muscle atrophy.

Increasing numbers of lncRNAs have been identified as important regulators of muscle development, muscle regeneration, and muscle wasting.[27–29] In this study, we revealed the novel function of *SYISL* in muscle atrophy and found that *SYISL* promotes muscle atrophy through FoxO signalling pathways and ubiquitin-mediated proteolysis. *SYISL* KO or knockdown could alleviate sarcopenia in aged mice. Sarcopenia is a serious muscle wasting disease; it also incurs a substantial economic burden related to medical costs.[30–32] Currently, targeting of muscular dystrophy-related pathways (e.g. myostatin/TGF-β/activin scavengers or bone morphogenetic protein agonists,[33] IGF-1 signalling,[34] β2-adrenoreceptor agonists,[35] and inhibitors of the UPS[36]) has become an important therapeutic strategy for sarcopenia. To explore the possibility of *SYISL* as a therapeutic target for sarcopenia, we investigated whether *hSYISL* could regulate muscle atrophy. The results suggest that targeting of *SYISL* is a promising novel therapeutic strategy for muscle atrophy and sarcopenia.

LncRNAs can function in various manners, such as binding to chromosomal modification complexes and transcription factors, and serve as molecular sponges for miRNAs.[37] Our study demonstrated that sponging of *miR-23a-3p*, *miR-103-3p*, and *miR-205-5p* by *SYISL* attenuates the inhibitory effects of these miRNAs on target gene expression and muscle atrophy. *miR-23a-3p* targets *MuRF1* and *Atrogin-1* and inhibits muscle atrophy.[22] Moreover, multiple reports have described sponging of *miR-103-3p* and *miR-205-5p*, mainly in the context of cancer.[38,39] However, the effects of *miR-103-3p* and *miR-205-5p* on muscle atrophy have been unclear. Here, we found that *miR-103-3p* and *miR-205-5p* inhibit muscle atrophy by targeting *MuRF1* and *FoxO3a*; sponging of miRNAs by *SYISL* weakens the inhibitory effects of *miR-103-3p* and *miR-205-5p* on target gene expression. Thus, miRNA sponging is the main mechanism by which *SYISL* regulates muscle atrophy; *miR-23a-3p*, *miR-103-3p*, and *miR-205-5p* function cooperatively in this process.

In summary, we identified *SYISL* homologues in humans and pigs; we found that the *SYISL*-mediated regulation of myogenesis is conserved among mice, pigs, and humans. Comparative analysis of *SYISL* in mice, pigs, and humans revealed its novel function in muscle atrophy and sarcopenia. Mechanistic analysis showed that *SYISL* simultaneously binds to *miR-23a-3p*, *miR-103-3p*, and *miR-205-5p*; it promotes muscle atrophy by attenuating their inhibitory effects on the expression levels of the muscle atrophy-related genes *MuRF1*, *Atrogin-1*, and *FoxO3a*. In addition, we verified that human *SYISL* accelerates muscle atrophy via conserved mechanisms. Our study provides novel perspectives regarding potential therapeutic targets for muscle atrophy and sarcopenia.

Acknowledgements

Online supplementary material

Additional supporting information may be found online in the Supporting Information section at the end of the article.

Conflict of interest

The authors declare no conflict of interest.

References

1. Egerman MA, Glass DJ. Signaling pathways controlling skeletal muscle mass. *Crit Rev Biochem Mol Biol* 2014;**49**: 59–68.

2. Sartori R, Romanello V, Sandri M. Mechanisms of muscle atrophy and hypertrophy: implications in health and disease. *Nat Commun* 2021;**12**:330.

3. Larsson L, Degens H, Li M, Salviati L, Lee YI, Thompson W, et al. Sarcopenia: aging-related loss of muscle mass and function. *Physiol Rev* 2019;**99**:427–511.

4. von Haehling S, Ebner N, Dos Santos MR, Springer J, Anker SD. Muscle wasting and cachexia in heart failure: mechanisms and therapies. *Nat Rev Cardiol* 2017;**14**: 323–341.

5. Cohen S, Nathan JA, Goldberg AL. Muscle wasting in disease: molecular mechanisms and promising therapies. *Nat Rev Drug Discov* 2015;**14**:58–74.

6. Sandri M. Protein breakdown in muscle wasting: role of autophagy-lysosome and ubiquitin-proteasome. *Int J Biochem Cell Biol* 2013;**45**:2121–2129.

7. Mitch WE, Goldberg AL. Mechanisms of muscle wasting. The role of the ubiquitin-proteasome pathway. *N Engl J Med* 1996;**335**:1897–1905.

8. Bodine SC, Baehr LM. Skeletal muscle atrophy and the E3 ubiquitin ligases MuRF1 and MAFbx/atrogin-1. *Am J Physiol Endocrinol Metab* 2014;**307**:E469–E484.

9. Masiero E, Agatea L, Mammucari C, Blaauw B, Loro E, Komatsu M, et al. Autophagy is required to maintain muscle mass. *Cell Metab* 2009;**10**:507–515.

10. Wiedmer P, Jung T, Castro JP, Pomatto LCD, Sun PY, Davies KJA, et al. Sarcopenia—molecular mechanisms and open questions. *Ageing Res Rev* 2021;**65**:101200.

11. Glass DJ. Signalling pathways that mediate skeletal muscle hypertrophy and atrophy. *Nat Cell Biol* 2003;**5**:87–90.

12. Milan G, Romanello V, Pescatore F, Armani A, Paik JH, Frasson L, et al. Regulation of autophagy and the ubiquitin-proteasome system by the FoxO transcriptional network during muscle atrophy. *Nat Commun* 2015;**6**:6670.

13. Sandri M, Sandri C, Gilbert A, Skurk C, Calabria E, Picard A, et al. Foxo transcription factors induce the atrophy-related ubiquitin ligase atrogin-1 and cause skeletal muscle atrophy. *Cell* 2004;**117**:399–412.

14. Kopp F, Mendell JT. Functional classification and experimental dissection of long noncoding RNAs. *Cell* 2018;**172**:393–407.

15. Ransohoff JD, Wei Y, Khavari PA. The functions and unique features of long intergenic non-coding RNA. *Nat Rev Mol Cell Biol* 2018;**19**:143–157.

16. Wang S, Zuo H, Jin J, Lv W, Xu Z, Fan Y, et al. Long noncoding RNA Neat1 modulates myogenesis by recruiting Ezh2. *Cell Death Dis* 2019;**10**:505.

17. Zhou L, Sun K, Zhao Y, Zhang S, Wang X, Li Y, et al. Linc-YY1 promotes myogenic differentiation and muscle regeneration through an interaction with the transcription factor YY1. *Nat Commun* 2015;**6**:10026.

18. Dey BK, Pfeifer K, Dutta A. The H19 long noncoding RNA gives rise to microRNAs miR-675-3p and miR-675-5p to promote skeletal muscle differentiation and regeneration. *Genes Dev* 2014;**28**:491–501.

19. Lv W, Jin J, Xu Z, Luo H, Guo Y, Wang X, et al. lncMGPF is a novel positive regulator of muscle growth and regeneration. *J Cachexia Sarcopenia Muscle* 2020;**11**: 1723–1746.

20. Jin JJ, Lv W, Xia P, Xu ZY, Zheng AD, Wang XJ, et al. Long noncoding RNA SYISL regulates myogenesis by interacting with polycomb repressive complex 2. *Proc Natl Acad Sci U S A* 2018;**115**:E9802–E9811.

21. Rion N, Castets P, Lin S, Enderle L, Reinhard JR, Eickhorst C, et al. mTOR controls embryonic and adult myogenesis via mTORC1. *Development* 2019;**146**.

22. Hudson MB, Woodworth-Hobbs ME, Zheng B, Rahnert JA, Blount MA, Gooch JL, et al. miR-23a is decreased during muscle atrophy by a mechanism that includes calcineurin signaling and exosome-mediated export. *Am J Physiol Cell Physiol* 2014;**306**: C551–C558.

23. Nitsche A, Stadler PF. Evolutionary clues in lncRNAs. *Wiley Interdiscip Rev RNA* 2017;**8**: e1376.

24. Li J, Zhao W, Li Q, Huang Z, Li C. Long non-coding RNA H19 promotes porcine satellite cell differentiation by interacting with TDP43. *Genes* 2020;**11**:259.

25. Maenner S, Blaud M, Fouillen L, Savoye A, Marchand V, Dubois A, et al. 2-D structure of the A region of Xist RNA and its implication for PRC2 association. *PLoS Biol* 2010;**8**: e1000276.

26. Sui B, Chen D, Liu W, Wu Q, Tian B, Li Y, et al. A novel antiviral lncRNA, EDAL, shields a T309 O-GlcNAcylation site to promote EZH2 lysosomal degradation. *Genome Biol* 2020;**21**:228.

27. Li Z, Cai B, Abdalla BA, Zhu X, Zheng M, Han P, et al. LncIRS1 controls muscle atrophy via sponging miR-15 family to activate IGF1-PI3K/AKT pathway. *J Cachexia Sarcopenia Muscle* 2019;**10**:391–410.

28. Li J, Yang T, Tang H, Sha Z, Chen R, Chen L, et al. Inhibition of lncRNA MAAT controls multiple types of muscle atrophy by cis- and trans-regulatory actions. *Mol Ther* 2021;**29**:1102–1119.

29. Wang S, Jin J, Xu Z, Zuo B. Functions and regulatory mechanisms of lncRNAs in skeletal myogenesis, muscle disease and meat production. *Cells* 2019;**8**:1107.

30. Goates S, Du K, Arensberg MB, Gaillard T, Guralnik J, Pereira SL. Economic impact of hospitalizations in US adults with sarcopenia. *J Frailty Aging* 2019;**8**:93–99.

31. Steffl M, Sima J, Shiells K, Holmerova I. The increase in health care costs associated with muscle weakness in older people without long-term illnesses in the Czech Republic: results from the Survey of Health, Ageing and Retirement in Europe (SHARE). *Clin Interv Aging* 2017;**12**:2003–2007.

32. Xie WQ, He M, Yu DJ, Wu YX, Wang XH, Lv S, et al. Mouse models of sarcopenia: classification and evaluation. *J Cachexia Sarcopenia Muscle* 2021;**12**:538–554.

33. Golan T, Geva R, Richards D, Madhusudan S, Lin BK, Wang HT, et al. LY2495655, an antimyostatin antibody, in pancreatic cancer: a randomized, phase 2 trial. *J Cachexia Sarcopenia Muscle* 2018;**9**:871–879.

34. Porporato PE, Filigheddu N, Reano S, Ferrara M, Angelino E, Gnocchi VF, et al. Acylated and unacylated ghrelin impair skeletal muscle atrophy in mice. *J Clin Invest* 2013; **123**:611–622.

35. Goncalves DA, Silveira WA, Lira EC, Graca FA, Paula-Gomes S, Zanon NM, et al. Clenbuterol suppresses proteasomal and lysosomal proteolysis and atrophy-related genes in denervated rat soleus muscles independently of Akt. *Am J Physiol Endocrinol Metab* 2012;**302**:E123–E133.

36. Adams V, Bowen TS, Werner S, Barthel P, Amberger C, Konzer A, et al. Small-molecule-mediated chemical knock-down of MuRF1/MuRF2 and attenuation of diaphragm dysfunction in chronic heart failure. *J Cachexia Sarcopenia Muscle* 2019; **10**:1102–1115.

37. Chen LL. Linking long noncoding RNA localization and function. *Trends Biochem Sci* 2016;**41**:761–772.

38. Tao P, Yang B, Zhang H, Sun L, Zheng W. The overexpression of lncRNA MEG3 inhibits cell viability and invasion and promotes apoptosis in ovarian cancer by sponging miR-205-5p. *Int J Clin Exp Pathol* 2020;**13**:869–879.

39. He Q, Zhao L, Liu X, Zheng J, Liu Y, Liu L, et al. MOV10 binding circ-DICER1 regulates the angiogenesis of glioma via miR-103a-3p/miR-382-5p mediated ZIC4 expression change. *J Exp Clin Cancer Res* 2019;**38**:9.

40. von Haehling S, Morley JE, Coats AJS, Anker SD. Ethical guidelines for publishing in the *Journal of Cachexia, Sarcopenia and Muscle*: update 2021. *J Cachexia Sarcopenia Muscle* 2021;**12**:2259–2261.